

# Change Detection in Heterogeneous Remote Sensing Images Based on Multidimensional Evidential Reasoning

Zhun-ga Liu, Grégoire Mercier, Jean Dezert, and Quan Pan

**Abstract**—We present a multidimensional evidential reasoning (MDER) approach to estimate change detection from the fusion of heterogeneous remote sensing images. MDER is based on a multidimensional (M-D) frame of discernment composed by the Cartesian product of the separate frames of discernment used for the classification of each image. Every element of the M-D frame is a basic joint state that allows to describe precisely the possible change occurrences between the heterogeneous images. Two kinds of rules of combination are proposed for working either with the free model, or with a constrained model depending on the integrity constraints one wants to take into account in the scenario under study. We show the potential interest of the MDER approach for detecting changes due to a flood in the Gloucester area in the U.K. from two real ERS and SPOT images.

**Index Terms**—Belief functions, change detection, Dezert-Smarandache Theory (DSmT), Dempster-Shafer Theory (DST), remote sensing (RS).

## I. INTRODUCTION

**I**N CHANGE detection from heterogeneous remote sensing (RS) images, many works have been devoted to change measure [1]–[5]. Recent works have also been done on the classification of changed features [6]–[10]. Particularly, an unsupervised change detection approach has been proposed in [4] for dealing with multisource and multisensor remote sensing images that allows to integrate the estimates of statistical terms achieved on the difference images. In [5], the similarity between the predicted image obtained from optical image and the SAR image is used to detect the damages caused by an earthquake. The heterogeneous remote sensing images are usually acquired from different kinds of sensors. Therefore, the classification does not necessarily involve the same classes definition (i.e., surface roughness from radar

versus chlorophyll from optical sensor, etc.). Moreover, the images usually include uncertain information due to noises, and imprecise information due to lack of knowledge specially at the transition between areas [11]. The limited quality of information makes the detection of changes between heterogeneous remote sensing images difficult to accomplish. In this letter, the change detection is considered as a classification problem, and we envisage the fusion of the classified images as appropriate for the change detection in heterogeneous remote sensing images. The fusion of classified images requires efficient tools for working with uncertain, imprecise, and even conflicting pieces of information. The theories of Evidences, including the Dempster-Shafer Theory (DST) [12] and Dezert-Smarandache Theory (DSmT) [13] propose theoretical frameworks to deal with uncertain and imprecise information. These theories have already been applied for the fusion of remote sensing images [14], [15].

The classical DST framework is not well adapted for change detection between images. Indeed, all the conflicting masses of belief that could be used to detect the changes are added altogether in a total degree of conflict that enters in the normalization constant of Dempster-Shafer (DS) fusion rule. To overcome the flaws and limitations of DST and DS rule [16], [17], new possible modelings of the frame of discernment and rules of combination were proposed in DSmT [13] for dealing separately with all the partial conflicts. Unfortunately, for change detection in RS images, the partial conflicting elements do not model sufficiently well the change occurrences since the element  $A \cap B = B \cap A$  cannot distinguish the change occurrences from  $A$  to  $B$  or from  $B$  to  $A$ . In our previous works [18], [19], a dynamic evidential reasoning (DER) approach had been developed for the change detection from RS images issued from the same type of remote sensor (e.g., a pair of SPOT images). In DER approach, the classes of these images were elements of the same frame of discernment. In this letter, we mainly focus on the change detection from the heterogeneous remote sensing images (e.g., from optical and radar images), where the classes of the images can be defined in distinct frames of discernments.

We propose a general multidimensional evidential reasoning (MDER) approach, which is effective for the change detection from both heterogeneous and homogenous remote sensing images. MDER is designed for the fusion of multisources classified images using same or dis-

Manuscript received October 24, 2012; revised January 7, 2013; accepted February 16, 2013. Date of publication April 8, 2013; date of current version November 8, 2013. This work was supported in part by the China Natural Science Foundation under Grants 61075029 and 61135001.

Z.-G. Liu is with the School of Automation, Northwestern Polytechnical University, Xi'an 710072, China, and also with Télécom Bretagne, Technopôle Brest-Iroise, Brest 29238, France (e-mail: liuzhunga@gmail.com).

G. Mercier is with Télécom Bretagne, Technopôle Brest-Iroise, Brest 29238, France (e-mail: gregoire.mercier@telecom-bretagne.eu).

J. Dezert is with Onera—The French Aerospace Laboratory, Palaiseau 91761, France (e-mail: jean.dezert@onera.fr).

Q. Pan is with the School of Automation, Northwestern Polytechnical University, Xi'an, China (e-mail: quanpan@nwpu.edu.cn).

Color versions of one or more of the figures in this paper are available online at <http://ieeexplore.ieee.org>.

Digital Object Identifier 10.1109/LGRS.2013.2250908

tinct frames of discernment depending on the classifications done on the images. MDER can be considered as an extension of classical evidential reasoning methods (DST, DSMT, and DER) for working under the multidimensional (M-D)<sup>1</sup> frame of discernment composed by the Cartesian product of the separate monodimensional (1-D) frames.<sup>2</sup> The elements of the M-D frame are called basic joint states. The space of the fusion result lies in the M-D power-set, which is constructed by the basic joint states with the union operator. The number of dimensions of the basic joint state depends on the number of images available. The joint states offer a better representation of the image mapping and change occurrences in the fusion of different images. The MDER approach provides a more refined information than what we get from the classical evidential reasoning approaches when working only in a 1-D frame. For dealing with different situations encountered in real applications, we provide two rules of combination adapted for the free and the constrained models of the M-D frame of discernment.

Section II details the framework of MDER, while Section III focuses on the combination rules that allows the classification of heterogeneous data, as well as the change detection from a set of heterogeneous data. Section IV presents an application of MDER using real heterogeneous data (i.e., SPOT and ERS images). Conclusions and perspectives are given in Section V.

## II. MULTIDIMENSIONAL EVIDENTIAL REASONING FRAMEWORK

### A. Space of Multidimensional Evidential Reasoning

In the MDER approach, the fusion space is always increasing with the number of sources, no matter if the 1-D frames of the sources to combine are identical or not. Even if the sources of evidence obtained from each image are respectively defined in 1-D frames, their fusion results will be considered in M-D frame defined by the Cartesian product of these 1-D frames to better represent the joint state of the heterogeneous images.

Let us consider  $n$  sources of evidence respectively defined with respect to  $n$  1-D frames  $\Theta_1, \Theta_2, \dots, \Theta_n$ . The frame of classifications of the  $i$ th image ( $i = 1, \dots, n$ ) is  $\Theta_i = \{y_{i,1}, y_{i,2}, \dots, y_{i,h_i}\}$ , where elements  $y_{i,k}, k = 1, \dots, h_i$  are the classes available in the  $i$ th image. The frames  $\Theta_i$  and  $\Theta_j, i \neq j$  can be similar, or different depending on the classifications done in each image. The M-D frame is  $\Psi^n \triangleq \Theta_1 \times \Theta_2 \times \dots \times \Theta_n$ , where symbols  $\times$  denotes the Cartesian product operator, and  $\triangleq$  means equals by definition. The cardinality of  $\Psi^n$  is  $|\Psi^n| = |\Theta_1| \times |\Theta_2| \times \dots \times |\Theta_n|$ , where  $|X|$  being the cardinality of  $X$  is the number of singletons in  $X$ . The M-D element  $(y_1, y_2, \dots, y_n) \in \Psi^n$  is called the basic joint-state of different images, with the interpretation that in the same region of  $n$  sources of coregistered multitemporal images, the content of this region in the image number  $i$  belongs to  $y_i$ , for  $i = 1, \dots, n$ . The fusion space of MDER is given by the power set of the product frame, which is

<sup>1</sup>M-D means that the elements are obtained from multiple frames of discernment.

<sup>2</sup>1-D here means that the elements are all from the same unique frame of discernment

$2^{\Psi^n} = 2^{\Theta_1 \times \Theta_2 \times \dots \times \Theta_n}$ . The M-D power-set  $2^{\Psi^n}$  is composed by all the subsets of  $\Psi^n$ . The cardinality of  $2^{\Psi^n}$  is  $|2^{\Psi^n}| = 2^{|\Psi^n|} = 2^{|\Theta_1| \times |\Theta_2| \times \dots \times |\Theta_n|}$ . In MDER approach, the operators  $\cup$  and  $\cap$  applied to elements  $A, B \in 2^{\Theta_1}$ , and  $C, D \in 2^{\Theta_2}$  must satisfy the following conditions:

C1) Componentwise distributivity of union:

$$(A \cup B, C \cup D) = (A, C) \cup (A, D) \cup (B, C) \cup (B, D)$$

C2) Componentwise intersection:

$$(A, C) \cap (B, D) = (A \cap B, C \cap D)$$

C3) Vacuity of joint states:  $(A, \emptyset) = (\emptyset, A) = \emptyset$ .

### B. Basic Definitions

In the MDER approach, a basic belief assignment (bba) is defined as a function  $m(\cdot)$  from the M-D power-set  $2^{\Psi^n}$  to  $[0, 1]$ , verifying  $m(\emptyset) = 0$  and

$$\sum_{A \in 2^{\Psi^n}} m(A) = 1. \quad (1)$$

Any element  $A \in 2^{\Psi^n}$  such that  $m(A) > 0$  is called a M-D focal element of  $m(\cdot)$ . All the imprecise joint states can be decomposed in the canonical disjunctive form using the basic joint states with the operator  $\cup$  according to the condition C1. For example,  $(X \cup Y, Z) = (X, Z) \cup (Y, Z)$ . With the canonical disjunctive form of the joint states, the belief  $\text{Bel}(\cdot)$  and plausibility  $\text{Pl}(\cdot)$  functions are defined by

$$\text{Bel}(A) = \sum_{A, B \in 2^{\Psi^n} | B \subset A} m(B) \quad (2)$$

$$\text{Pl}(A) = \sum_{A, B \in 2^{\Psi^n} | A \cap B \neq \emptyset} m(B). \quad (3)$$

The interval  $[\text{Bel}(A), \text{Pl}(A)]$  is classically interpreted [12] as the lower and upper bounds of imprecise probability for decision-making support. The pignistic probability  $\text{BetP}(A)$  [20] commonly used to approximate the unknown probability in  $[\text{Bel}(A), \text{Pl}(A)]$  is calculated by

$$\text{BetP}(A) = \sum_{B \in 2^{\Psi^n}, B \neq \emptyset} \frac{|A \cap B|}{|B|} m(B). \quad (4)$$

In MDER, the cardinality of  $A \in 2^{\Psi^n}$  is the number of the basic joint states contained in the canonical disjunctive form of  $A$ .

*Example 1:* Let us consider the following bba's over  $\Psi^2 = \Theta \times \Omega$  with  $\Theta = \{\theta_1, \theta_2\}$  and  $\Omega = \{\omega_1, \omega_2, \omega_3\} : m(\theta_1, \omega_2) = 0.5, m(\theta_1, \omega_2 \cup \omega_3) = 0.2$  and  $m(\Theta, \omega_3) = 0.3$ . The cardinality of the imprecise joint states is counted as follows:

$$|(\theta_1, \omega_2 \cup \omega_3)| = |(\theta_1, \omega_2) \cup (\theta_1, \omega_3)| = 2$$

$$|(\Theta, \omega_3)| = |(\theta_1 \cup \theta_2, \omega_3)| = |(\theta_1, \omega_3) \cup (\theta_2, \omega_3)| = 2$$

Then one gets  $\text{Bel}(\theta_1, \omega_3) = \text{Bel}(\theta_2, \omega_3) = 0$  and

$$\begin{aligned} \text{Bel}(\theta_1, \omega_2) &= m(\theta_1, \omega_2) = 0.5 \\ \text{Pl}(\theta_1, \omega_2) &= m(\theta_1, \omega_2) + m(\theta_1, \omega_2 \cup \omega_3) = 0.7 \\ \text{Pl}(\theta_1, \omega_3) &= m(\theta_1, \omega_2 \cup \omega_3) + m(\Theta, \omega_3) = 0.5 \\ \text{Pl}(\theta_2, \omega_3) &= m(\Theta, \omega_3) = 0.3 \\ \text{BetP}(\theta_1, \omega_2) &= m(\theta_1, \omega_2) + \frac{m(\theta_1, \omega_2 \cup \omega_3)}{2} = 0.6 \\ \text{BetP}(\theta_1, \omega_3) &= \frac{m(\theta_1, \omega_2 \cup \omega_3)}{2} + \frac{m(\Theta, \omega_3)}{2} = 0.25 \\ \text{BetP}(\theta_2, \omega_3) &= \frac{m(\Theta, \omega_3)}{2} = 0.15. \end{aligned}$$

### III. COMBINATION RULES IN MULTIDIMENSIONAL EVIDENTIAL REASONING

In DST [12] or in DSMT [13], the source of evidence provide their bba's defined on a same frame of discernment, and a particular attention is focused on the way in which the conflicting masses of belief are redistributed. In the DER approach [18], the sources of evidences are also defined on the same frame of discernment and they are sequentially combined. In the change detection of heterogenous images, the classes of each image source can be defined in the distinct frames of discernment because the sets of classes can be different from one image to another. To deal with this problem, we propose to combine the sources of evidence in the M-D frame constructed by the Cartesian product of the distinct 1-D frames. By doing this, we exploit more efficiently the information in the fusion process, and thus we can estimate more precisely the changes between the images, taking into account the integrity constraints (if any) of the model of the M-D frame.

Let us consider  $n$  sources of heterogeneous images to be fused, and let us assume that the classifications of each image are respectively defined over the frames  $\Theta_1, \dots, \Theta_n$ . The bba's obtained from each image at the same region are combined as  $m(\cdot) = [m_1 \oplus m_2 \oplus \dots \oplus m_n](\cdot)$ , where  $\oplus$  denotes the generic fusion operator. Before applying the fusion of sources, the original bba  $m_i(\cdot)$  associated with the  $i$ -th image (for  $i = 1, 2, \dots, n$ ) needs to be extended to joint states representation in the M-D frame using the vacuous extension principle [21] as follows:

$$m_i(A) \triangleq m_i(\Theta_1, \dots, \Theta_{i-1}, A, \Theta_{i+1}, \dots, \Theta_n). \quad (5)$$

This method is called the vacuous extension because we do not use information provided by the other sources to extend  $m_i(A)$  in the M-D frame. Such vacuous extension is very simple since it does not take into account the temporal correlation among images. The prior knowledge of the temporal correlation (if available, depending on the applications) can be taken into account in the fusion process to improve the performances of multitemporal classification and change detection.

Two combination models are proposed here. The free combination model is applied if no prior knowledge about the impossible joint states is known. Whereas, the constrained combination should be used when some integrity constraints on the joint states must be taken into account.

#### A. Combination Rule in the Free Model

In the free model, all elements (joint states) of  $2^{\Psi^n}$  are allowed to occur. Thus, there is no element that is forced to be impossible.<sup>3</sup> At first, the bba's drawn from the classifications done on the images are extended into the M-D frame using the vacuous extension following (5). Then the conjunctive combination rule, denoted  $\text{MDER}_f$ , of the extended bba's in the M-D frame is defined  $\forall A, Y_i \in 2^{\Psi^n}$  by

$$\text{MDER}_f : \quad m(A) = \prod_{\substack{i=1 \\ Y_1 \cap Y_2 \cap \dots \cap Y_n = A}}^n m_i(Y_i) \quad (6)$$

The mass  $m(A)$  obtained in (6) can also be computed by the sequential fusion of the  $n \geq 2$  original (one dimension) bba's as follows for  $A = (Y, y_n) \in 2^{\Psi^n}$

$$m_{1 \oplus \dots \oplus n}(A) = m_{1 \oplus \dots \oplus n-1}(Y) m_n(y_n) \quad (7)$$

where  $Y = (y_1, y_2, \dots, y_{n-1}) \in 2^{\Psi^{n-1}}$  and

$$\begin{cases} m_{1 \oplus \dots \oplus n-1}(\cdot) \triangleq [m_1 \oplus m_2 \oplus \dots \oplus m_{n-1}](\cdot) \\ m_{1 \oplus}(\cdot) \triangleq m_1(\cdot). \end{cases} \quad (8)$$

#### B. Combination Rule in the Constrained Model

In some applications, particular joint states in  $2^{\Psi^n}$  are known impossible to happen (e.g., a forest seen by a first sensor that appears without any roughness by a latter radar sensor). All these impossible joint states are therefore constrained to be represented by the empty set. The set of all the integrity constraints is denoted  $\emptyset_{\mathcal{M}}$ . The mass of the empty sets forced by the integrity constraints has to be redistributed to the other focal elements of  $2^{\Psi^n}$ . Several redistribution principles can be adopted. In this letter, we propose to redistribute the conflicting masses to the focal elements, thanks to the classical normalization procedure adopted in DS rule, because of its simplicity.<sup>4</sup> The combination of  $n$  bba's, denoted  $\text{MDER}_{\text{DS}}$ , is defined by  $\forall A \in 2^{\Psi^n}$

$$\text{MDER}_{\text{DS}} : \quad m(A) = \frac{1}{1 - K} \sum_{(y_1, \dots, y_n) \stackrel{\mathcal{M}}{=} A} \prod_{i=1}^n m_i(y_i) \quad (9)$$

where  $y_i \in 2^{\Theta_i}$ ,  $i = 1, \dots, n$ , and the total conflicting mass  $K$  is defined by

$$K = \sum_{(y_1, \dots, y_n) \in \emptyset_{\mathcal{M}}} m_1(y_1) \cdots m_n(y_n). \quad (10)$$

The notation  $(y_1, y_2, \dots, y_n) \stackrel{\mathcal{M}}{=} Y$ , means that the hypothesis  $(y_1, y_2, \dots, y_n)$  is equivalent to  $Y$  in the underlying model  $\mathcal{M}$  given the integrity constraints. For example, if we have the constraint  $(y_{1;i}, y_{2;j}) \in \emptyset_{\mathcal{M}}$  in a 2-D framework, then the joint state  $(y_{1;i}, y_{2;j} \cup y_{2;k})$  can be simplified as  $(y_{1;i}, y_{2;j} \cup y_{2;k}) = (y_{1;i}, y_{2;j}) \cup (y_{1;i}, y_{2;k}) = \emptyset \cup (y_{1;i}, y_{2;k}) = (y_{1;i}, y_{2;k})$ .

<sup>3</sup>The impossible event is represented by the empty set in DST and DSMT.

<sup>4</sup> $\text{MDER}$  is a general framework that can be used with different rules of combinations. We only propose a DS alike fusion rule for  $\text{MDER}$  here for its relatively low complexity, but other rules as in [13, vol. 2] can also be used.

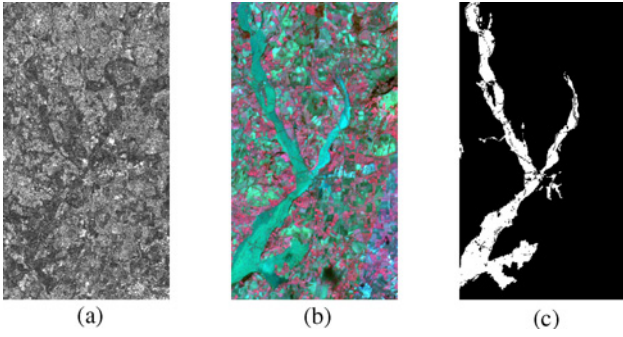


Fig. 1. ERS and SPOT images of Gloucester U.K. (a) ERS image, acquired on November 16, 1999 before the flood. (b) SPOT image, acquired on October 21, 2000 during the flood. (c) Ground truth.

All the bba's defined with respect to a 1-D frame can also be (vacuously) extended to M-D frame using (5) at first, and then they are combined with a proper redistribution of conflicting beliefs.

#### IV. APPLICATION OF MDER ON ERS AND SPOT IMAGES

In this section, we show the performances of  $\text{MDER}_{\text{DS}}$  for the change detection between a pair of heterogenous images (an ERS and a SPOT image) obtained before and immediately after a flood in Gloucester area in U.K. The ERS and Spot images are shown in Fig. 1, as well as the binary image of the ground truth.

We want to focus on the application of MDER on fusion of the classified images, and the appropriate classification method can be selected according to the actual applications. The classification of images plays a basic role in change detections problem, and the more accurate classification results lead to the better fusion results using MDER or other approaches. A very recent clustering method called belief functions C-means (BFCM) [22] as an extension of Fuzzy C-means (FCM) under belief functions framework can well model the imprecision and uncertainty. BFCM is applied to classify the pixel values of each pixel of the images, and its results can be directly used as bba's. For decision making, the maximum pignistic probability is used to select the most likely hypothesis.

The number of clusters for ERS image despeckled by a refined Lee filter [23] with a  $7 \times 7$  sliding window is given by  $k_{\text{ERS}} = 3$ . The classification results are defined in the frame as [from lower to higher level of surface roughness in Fig. 1(a)] follows:

$$\begin{aligned} \theta_1 &\triangleq \text{Dark area} & \theta_2 &\triangleq \text{Gray area} \\ \theta_3 &\triangleq \text{White area} & \Theta &\triangleq \text{Ignorance.} \end{aligned}$$

The SPOT image in Fig. 1(b) was clustered into  $k_{\text{SPOT}} = 5$  groups of possible classes as listed below:

$$\begin{aligned} \omega_1 &\triangleq \text{Red area (covered fields)} \\ \omega_2 &\triangleq \text{Dark-red area (wooded area)} \\ \omega_3 &\triangleq \text{Green area (bare soil)} \\ \omega_4 &\triangleq \text{Dark-green area (vegetation)} \\ \omega_5 &\triangleq \text{Bright-green area (bare soil and wet area)} \\ \Omega &\triangleq \text{Ignorance.} \end{aligned}$$

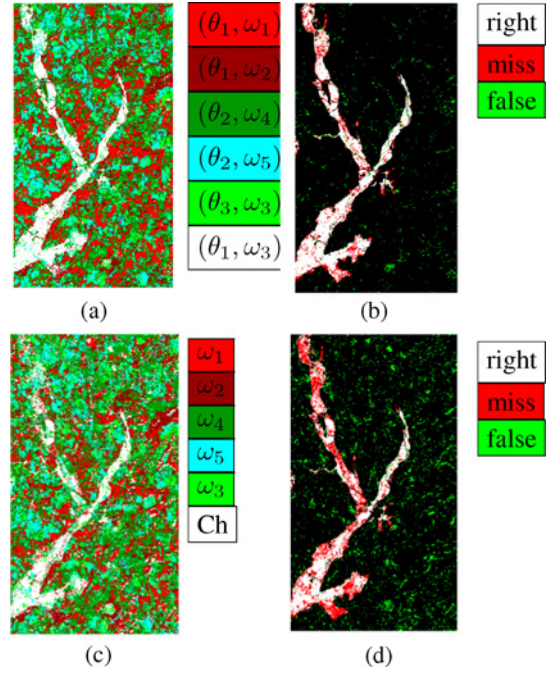


Fig. 2. Fusion results of the pair of ERS and SPOT images: (a) Fusion results by  $\text{MDER}_{\text{DS}}$ . (b) Comparison of the change detections with ground truth by  $\text{MDER}_{\text{DS}}$ . (c) Fusion results by DS<sub>m</sub>C (Ch denotes the change occurrences). (d) Comparison of the change detections with ground truth by DS<sub>m</sub>C.

The class that each cluster corresponds to is identified according to the clustering center. The cluster corresponds to the class of content whose pixel value is most close to the vector of this clustering center. For example, in the SPOT image, the related distance is the Euclidean distance in  $\mathbb{R}^3$  to the spectral signature that characterizes the class center. The related colors refer to the pseudo-color composition Near Infrared, Red, Green showed as red, green, blue colors. In ERS image, which has been filtered, the distance to cluster refers to the Euclidean distance in  $\mathbb{R}$  and the level of radiometry (from dark to white) is related to surface roughness (from  $\theta_1$  to  $\theta_3$ ).

The constrained model is used since we have some prior knowledge about this region in the image. The covered fields  $\omega_1$  and wooded area  $\omega_2$  are linked with low roughness  $\theta_1$ , and the bare soils  $\omega_3$  are linked with high roughness  $\theta_3$  in the ERS observation. The vegetation  $\omega_4$  and the wet area  $\omega_5$  mainly correspond to the gray area  $\theta_2$  in Fig. 1(a). Thus, one has five consistent joint states  $(\theta_1, \omega_1)$ ,  $(\theta_1, \omega_2)$ ,  $(\theta_3, \omega_3)$ ,  $(\theta_2, \omega_4)$ , and  $(\theta_2, \omega_5)$ . We also know that the change mainly occurred around the flooding zone. The flood destroyed the wooded area with low roughness  $\theta_1$ , and changed it to bare soil  $\omega_3$ . Therefore, the change occurrence mainly corresponds to the inconsistent joint state  $(\theta_1, \omega_3)$ . As a result, we select the five consistent joint states and one inconsistent joint state here.

DS<sub>m</sub>T has already been applied for change detection of RS images in [14]. To compare the combination rule DS<sub>m</sub>C [13] with  $\text{MDER}_{\text{DS}}$ ,<sup>5</sup> we mapped the frame  $\Theta$  to  $\Omega$  as  $\theta_1 \triangleq \{\omega_1, \omega_2\}$ ,  $\theta_2 \triangleq \{\omega_4, \omega_5\}$ ,  $\theta_3 \triangleq \{\omega_3\}$ . As for the change detection, one has  $\theta_1 \cap \omega_3 \triangleq (\omega_1 \cup \omega_2) \cap \omega_3 = (\omega_1 \cap \omega_3) \cup (\omega_2 \cap \omega_3)$ . So both  $\omega_1 \cap \omega_3$  and  $\omega_2 \cap \omega_3$  will be considered as the useful

<sup>5</sup>DS<sub>m</sub>C is the simple conjunctive rule, and all the possible conjunction between elements are allowed in this letter.

TABLE I  
PERFORMANCES OF THE MDER FUSION RESULTS (IN %)

	$R_a$	$R_m$	$R_f$	$K_a$
DSmC	65.52	42.46	34.48	55.65
MDER <sub>DS</sub>	81.80	16.53	18.20	80.30

conflict element representing the change occurrences. All the other conflict elements are constrained to be empty in the integrity model, and the conflicting beliefs are proportionally redistributed to the available elements similarly to the DS rule. The fusion results by different rules are shown in Fig. 2.

As a measure of performance, we use the accuracy rate  $R_a = n_a/N_d$ , the missing rate  $R_m = n_m/N_c$ , the false alarm rate  $R_f = n_f/N_d$ , and the Kappa index  $K_a$ .  $n_a$  is the number of pixels of correct change detections,  $N_d$  is the total number of pixels of detected changes,  $n_m$  is the number of pixels of nondetected changes,  $N_c$  is the total number of pixels of changes in ground truth, and  $n_f$  is the number of pixels of false alarms. The performances obtained by MDER<sub>DS</sub> and DSmC are listed in Table I.

As we can see, MDER<sub>DS</sub> provides much better fusion results than DSmC because DSmC produces more false alarms than MDER<sub>DS</sub> since the intersection element cannot precisely represent the change occurrences. The Kappa index can comprehensively reflect the quality of the classification results with respect to the change detections. So MDER<sub>DS</sub> has better quantitative performance than DSmC according to the  $K_a$  value. However, a fine analysis of results indicates that some missed detections and false alarms have also occurred. Our results show that gray and white areas along the river remain mainly consistent with green areas between the two images. So they are not considered as change occurrences, which mainly leads to the miss detections. The reason for the false alarms mainly lies in changes in some small areas that resemble to some changes in the flood area. The number of the false alarms can be reduced if additional prior information about the location of the flood is taken into account.

## V. CONCLUSION AND PERSPECTIVES

A MDER approach was proposed for the fusion of the heterogeneous remote sensing images. The multidimensional elements in MDER could well represent the joint states of different images, which was useful for change detection. The belief function, plausibility function, and pignistic probability in MDER were defined similarly as in DST. The free model of MDER was designed for the combination of sources of evidence, in cases, where no prior knowledge about the joint states was available. If some constraints on the impossible joint states were acquired, the constrained model has to be adopted to get better fusion results with less computational complexity. MDER<sub>DS</sub> rule was presented in the constrained model as a direct extension of DS rule in MDER. The capacity of MDER to detect and to classify change occurrences was also presented by a pair of real images (i.e., ERS and SPOT). MDER could also be used for the heterogeneous images mapping applications, and the experiments were under progress, as well as investigations on the use of other fusion rules based on the proportional conflict redistribution principle proposed in DSmT.

## REFERENCES

- [1] G. Mercier, G. Moser, and S. Serpico, "Conditional copulas for change detection in heterogeneous remote sensing images," *IEEE Trans. Geosci. Remote Sens.*, vol. 46, no. 5, pp. 1428–1441, May 2008.
- [2] G. Mercier, "Progressive change detection in time series of SAR images," in *Proc. IEEE Int. Geosci. Remote Sens. Symp.*, Honolulu, HI, USA, Jul. 2010, pp. 3086–3089.
- [3] A. Robin, G. Mercier, G. Moser, and S. Serpico, "An a contrario approach for unsupervised change detection in radar images," in *Proc. IEEE Int. Geosci. Remote Sens. Symp.*, vol. 4, Jul. 2009, pp. 197–204.
- [4] L. Bruzzone and D. Prieto, "Unsupervised change detection in multi-source and multisensor remote sensing images," in *Proc. Int. Geosci. Remote Sens. Symp.*, vol. 6, Honolulu, HI, USA, Jul. 2000, pp. 2441–2443.
- [5] B. Dominik, L. Guido, and L. Bruzzone, "Earthquake damage assessment of buildings using vhr optical and sar imagery," *IEEE Trans. Geosci. Remote Sens.*, vol. 48, no. 5, pp. 2403–2420, May 2010.
- [6] G. Moser, S. B. Serpico, and G. Vernazza, "Unsupervised change detection from multichannel SAR images," *IEEE Geosci. Remote Sens. Lett.*, vol. 4, no. 2, pp. 278–282, Apr. 2007.
- [7] F. Bovolo, L. Bruzzone, and M. Marconcini, "A novel approach to unsupervised change detection based on a semisupervised SVM and a similarity measure," *IEEE Trans. Geosci. Remote Sens.*, vol. 46, no. 7, pp. 2070–2082, Jul. 2008.
- [8] G. Moser and S. Serpico, "Unsupervised change detection from multichannel SAR data by markovian data fusion," *IEEE Trans. Geosci. Remote Sens.*, vol. 47, no. 7, pp. 2114–2128, Jul. 2009.
- [9] Y. Bazi, F. Melgani, and H. Al-Sharari, "Unsupervised change detection in multispectral remotely sensed imagery with level set methods," *IEEE Trans. Geosci. Remote Sens.*, vol. 48, no. 8, pp. 3178–3187, Aug. 2010.
- [10] T. Celik, "Change detection in satellite images using a genetic algorithm approach," *IEEE Geosci. Remote Sens. Lett.*, vol. 7, no. 2, pp. 386–390, Apr. 2010.
- [11] B. Lelandais, I. Gardin, L. Mouchard, P. Vera, and S. Ruan, "Using belief function theory to deal with uncertainties and imprecisions in image processing," in *Proc. 2nd Int. Conf. Belief Funct.*, Compiègne, France, May 2012.
- [12] G. Shafer, *A Mathematical Theory of Evidence*. Princeton, NJ, USA: Princeton Univ. Press, 1976.
- [13] F. Smarandache and J. Dezert, Eds. *Advances and Applications of DSmT for Information Fusion*, vol. 1–3. Rehoboth, NM, USA: American Research Press, 2009.
- [14] A. Bouakache, A. Belhadj-Aissa, and G. Mercier, "Satellite image fusion using Dezert–Smarandache theory," in *Advances and Applications of DSmT for Information Fusion*, vol. 3, F. Smarandache and J. Dezert, Eds. Rehoboth: NM, USA: ARP, 2009, ch. 22.
- [15] S. L. Hegarat-Masclé, I. Bloch, and D. Vidal-Madjar, "Application of Dempster–Shafer evidence theory to unsupervised classification in multisource remote sensing," *IEEE Trans. Geosci. Remote Sens.*, vol. 35, no. 4, pp. 1018–1031, Apr. 1997.
- [16] J. Dezert, P. Wang, and A. Tchamova, "On the validity of Dempster–Shafer theory," in *Proc. 15th Int. Conf. Inform. Fusion*, Jul. 2012, pp. 655–660.
- [17] A. Tchamova and J. Dezert, "On the behavior of Dempster's rule of combination and the foundations of Dempster–Shafer Theory," in *Proc. 6th Int. Conf. Intell. Syst.*, Sep. 2012, pp. 108–113.
- [18] Z. Liu, J. Dezert, G. Mercier, and Q. Pan, "Dynamic evidential reasoning for change detection in remote sensing images," *IEEE Trans. Geosci. Remote Sens.*, vol. 50, no. 5, pp. 1955–1967, May 2012.
- [19] Z. Liu, J. Dezert, G. Mercier, Q. Pan, and Y. Cheng, "Change detection from remote sensing images based on evidential reasoning," in *Proc. 14th Int. Conf. Inform. Fusion*, Jul. 2011, pp. 1–8.
- [20] P. Smets, "Decision making in the TBM: The necessity of the pignistic transformation," *Int. J. Acad. Res.*, vol. 38, no. 2, pp. 133–147, Feb. 2005.
- [21] P. Smets, "Belief functions: The disjunctive rule of combination and the generalized Bayesian theorem," *Int. J. Acad. Res.*, vol. 9, no. 1, pp. 1–35, 1993.
- [22] Z. Liu, J. Dezert, Q. Pan, and Y. Cheng, "A new evidential c-means clustering method," in *Proc. 15th Int. Conf. Inform. Fusion*, Jul. 2012, pp. 239–246.
- [23] J. Lee, "Refined filtering of image noise using local statistics," *Comp. Graph. Image Process.*, vol. 15, no. 4, pp. 380–389, Apr. 1981.